

# Biochemical Modification of Streptavidin and Avidin: In Vitro and In Vivo Analysis

Scott F. Rosebrough and Donna F. Hartley

Department of Radiology, University of Rochester Medical Center, Rochester, New York

The high affinity streptavidin (or avidin)/biotin system is being investigated for imaging and radiotherapy procedures. Streptavidin (SA) and avidin exhibit markedly different pharmacokinetics, with avidin clearing from the blood much faster than SA. To optimize blood clearance kinetics, SA and avidin were biochemically modified and analyzed in vitro and in vivo. **Methods:** Galactose moieties were covalently attached to promote binding by hepatocyte galactose receptors and hasten SA clearance. To prolong avidin clearance, avidin was deglycosylated and/or neutralized by acetylation of its lysine amino acids. In vitro, the modified proteins were analyzed by isoelectric focusing, SDS polyacrylamide electrophoresis and a biotin binding saturation assay. The modified and native proteins were radiolabeled with  $^{131}\text{I}$  and injected into rabbits for pharmacokinetic, biodistribution and imaging analysis. **Results:** For SA, the resulting increase in blood clearance and liver accumulation was correlated to the amount of galactose bound to SA. For avidin, each type of modification increased its circulation time, with the slowest clearance resulting from a combination of deglycosylation and neutralization. **Conclusion:** Biochemical modification of SA and avidin resulted in altered pharmacokinetics compared to the native proteins. Modified SA or avidin, when cross-linked with a lesion-specific targeting agent, may be applicable for rapid two-step in vivo imaging techniques.

**Key Words:** streptavidin; avidin; biotin; in vivo imaging

**J Nucl Med 1996; 37:1380-1384**

The high affinity ( $K_d = 10^{-15}$  M), tetravalency and stability of streptavidin (SA) and avidin for biotin has been utilized in many biochemical and clinical techniques (1). These biotin-based methods enable both a signal amplification and a reduction in background activity. Avidin and SA are similar in protein subunit conformation and affinity for biotin; they differ however, in primary amino acid sequence, net charge, glycosylation and immune cross-reactivity (2). Avidin has exhibited nonspecific binding in vitro and in vivo. Avidin contains twice the number of the basic amino acids lysine and arginine compared to SA; therefore, the isoelectric point of avidin is  $\sim 10$  compared to  $\sim 7$  for SA. Approximately 10% of avidin's mass is due to its carbohydrates—mannose and N-acetylglucosamine (3,4). These sugars are not necessary for the stability and the high binding affinity of avidin for biotin (5), but may be a factor in vivo due to its potential to bind with sugar receptors present throughout the reticuloendothelial system (6-9). SA is void of carbohydrates. Radiolabeled SA and avidin exhibit different plasma pharmacokinetics (10-12). SA circulates similar to other proteins, whereas avidin clears quickly from the blood and accumulates in the liver and kidneys.

We are developing a rapid two-step procedure, utilizing monoclonal antibodies (MAbs) cross-linked to biochemically modified SA as the in vivo targeting moiety, followed by injection of radiobiotin. Biotin derivatives have been developed

for binding radionuclides suitable for gamma camera imaging and, for cancer, radiotherapy (13-18). The advantage of having the radionuclide on the small molecular weight biotin molecule, compared to the use of directly radiolabeled MAbs, is a reduction in background levels and dosimetry due to rapid clearance of biotin by the kidneys.

For a rapid two-step approach, the optimal targeting agent would circulate adequately for sufficient lesion accumulation, but would clear in a reasonably short time prior to the injection of radiobiotin. Hence, the competition of target-bound SA MAb with unbound SA-MAb for radiobiotin would be alleviated. In this study, SA and avidin were biochemically modified to optimize their blood clearance rates. Galactose receptors reside mainly on hepatocytes and have been utilized in a variety of diagnostic and therapeutic procedures (6,7,19-22). To increase blood clearance, galactose was conjugated to SA in increasing amounts and the resultant SA-galactose (SA-gal) moieties were analyzed both in vitro and in vivo. Avidin's extremely rapid blood clearance and in vivo stickiness result from its inherent positive charge and its mannose terminal sugars which may bind to mannose receptors present in the liver (i.e., Kupffer cells). Avidin was modified to prolong its blood clearance by: (a) deglycosylation with digestion by endoglycosidase-H, (b) decreasing its positive charge by neutralization of lysine amino acids and (c) by both deglycosylation and neutralization.

## MATERIALS AND METHODS

### Biochemical Modification of SA and Avidin

SA was solubilized in 0.05 M sodium phosphate/0.15 M NaCl buffer, pH 8.0 at a concentration of 10 mg/ml as determined spectrophotometrically ( $E_{280\text{ nm}}^{1\%} = 34.0$ ) (2). Alpha-D-galactopyranosyl-phenylisothiocyanate was solubilized in methanol and added to SA in molar incubation ratios of 10, 25 and 50 for overnight incubation at room temperature. The SA-galactose (SA-gal) samples were then centrifuged using Microcon-30 filters. SA-bound galactose ratios were determined indirectly by quantifying galactose concentrations in the ultrafiltrate by an anthrone colorimetric assay (23). Avidin was neutralized by acetylation of lysine amino acids by incubating acetic acid N-hydroxysuccinimide ester with 5 mg/ml avidin ( $E_{280\text{ nm}}^{1\%} = 15.4$ ) in 0.05 M sodium phosphate/0.15 M NaCl buffer, pH 8.0 at molar ratios of 10, 25, 50 and 75 for 1 hr at room temperature. For deglycosylation, 5 mg/ml avidin in 0.05 M sodium citrate, pH 5.5 buffer was digested with 0.1 unit per ml endoglycosidase-H for 18 hr at 37°C. For deglycosylated and neutralized avidin, avidin was deglycosylated following the same protocol. The solution was then washed with 0.05 M sodium phosphate/0.15 M NaCl pH 8.0 buffer on a Centricon-30 filter followed by the addition of acetic acid N-hydroxysuccinimide ester at a 50:1 molar ratio.

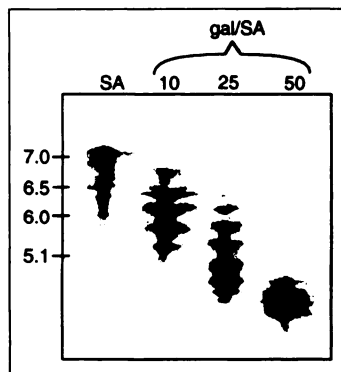
### Electrophoresis

Polyacrylamide isoelectric focusing was performed using a Bio Rad mini IEF cell (Bio Rad Labs, Hercules, CA) with ampholytes ranging from 3-8 pH or 3-10 pH for SA and avidin samples, respectively. SDS-polyacrylamide electrophoresis was performed

Received Mar. 29, 1995; revision accepted Jul. 29, 1995.

For correspondence or reprints contact: Scott F. Rosebrough, PhD, Department of Radiology, University of Rochester Medical Center, 601 Elmwood Ave., Box 648, Rochester, NY 14642.

**FIGURE 1.** Isoelectric focusing of SA and SA-gal showed a progressive decrease in isoelectric point with covalent attachment of galactose. Numbers indicate incubation ratios.



using a Bio Rad mini-Protein II cell with 17% polyacrylamide gels.

### Biotin Saturation Assay

Deferoxamineacetylcyteinylobiotin (DACB) has previously been developed by our group as a biotin containing chelate for in vitro and in vivo use with SA or avidin (15). DACB was radiolabeled by direct addition of carrier-free  $^{67}\text{Ga}$  citrate. Samples of SA, avidin and modified SA and avidin were incubated with a 20 to 1 molar excess of  $^{67}\text{Ga}$  DACB on Centricon-30 filters in 0.05 M Tris/0.15 M NaCl buffer, pH 7.5. After 2 washings, the bound DACB-to-protein ratio was determined by dividing the bound activity in the retentate by the specific activity of  $^{67}\text{Ga}$  DACB ( $\sim 2 \times 10^{16}$  cpm/mole). The binding ratios for each sample were determined by dividing the bound moles of DACB by the moles of each protein.

### Radiolabeling, Biodistribution and Imaging

SA, avidin and the modified proteins were radiolabeled with  $^{131}\text{I}$  by the Pierce Iodobead method (Pierce, Rockford, IL), and free iodine was removed by ultrafiltration using Centricon-30 filters. As previously reported (12), the labeling efficiency of SA was much better than that of avidin. Therefore, 0.5 mg SA and avidin were radiolabeled with starting activities of  $\sim 0.3$  mCi  $^{131}\text{I}$  and  $\sim 1$  mCi  $^{131}\text{I}$ , respectively. The radiolabeling yields were  $\sim 75\%$  for SA and  $\sim 25\%$  for avidin samples. When analyzed by Centricon-30 ultrafiltration, less than 5% free iodine was present in the injected samples.

All animal experiments were approved and conducted in facilities at the University of Rochester in compliance with the American Association for Accreditation of Laboratory Animal Care. New Zealand white rabbits,  $\sim 3$  kg, were fasted for 12 hr prior to experiment and anesthetized using an intramuscular injection of chlorpromazine (25 mg/kg) followed by intravenous sodium pentobarbital (15 mg/kg). For each animal, an external jugular vein was dissected and catheterized using a 5 French straight catheter for injection and collection of whole blood. The animal was placed in the supine position under the gamma camera for imaging and was injected with 75  $\mu\text{g}$  ( $\sim 30$   $\mu\text{Ci}$ ) of the radiolabeled protein. Whole blood samples (2–3 ml) were taken at intervals for 2 hr. Planar gamma camera images (30K count acquisition) were taken at 5, 30 and 120 min postinjection. At 2 hr postinjection, the animals were euthanized. Major organs were removed and weighed and representative samples were taken for biodistribution analysis by counting in a gamma counter. Blood volume was estimated to be 6% of total body weight (24,25).

### RESULTS

Galactose was covalently attached to SA via a nucleophilic reaction of SA's amino groups with alpha-D-galactopyranosylphenylisothiocyanate. Each conjugated galactose results in a decrease of one positive charge. Therefore, a progressive decrease in the isoelectric point of SA-gal samples incubated

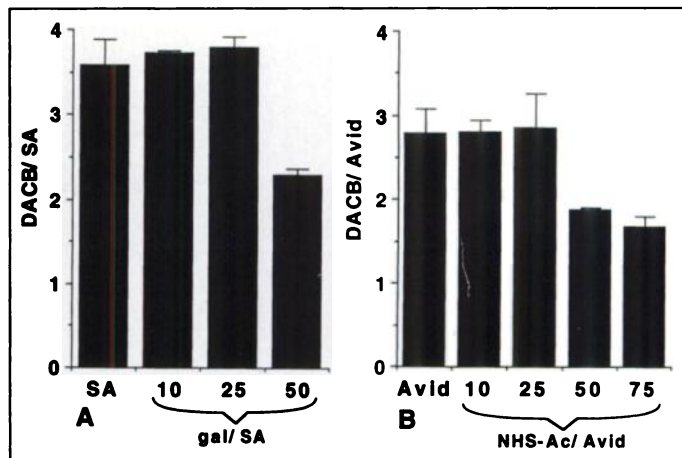


**FIGURE 2.** DACB saturation assay on SA, SA-gal, avidin and neutralized avidin. Abscissa-to-molar incubation ratios of galactose or NHS-Ac with protein. Ordinate-bound DACB/protein ratios ( $\bar{x} \pm \text{s.d.}$ ).

with galactose-to-SA molar ratios of 10, 25 and 50 was evident when analyzed by isoelectric focusing (Fig. 1). To evaluate SA-gal for biotin binding, each SA-gal sample was incubated with a molar excess of  $^{67}\text{Ga}$  DACB on Centricon-30 filters. After washing, the bound DACB-to-SA-gal ratio was determined by dividing the bound activity by the specific activity of  $^{67}\text{Ga}$  DACB (Fig. 2A). Control SA exhibited a binding ratio of 3.6, close to the tetrameric maximum binding. SA-gal samples with galactose-to-SA molar ratios of 10 and 25 exhibited no reduction in binding; the DACB saturation ratio for the gal-to-SA-50 sample, however, was reduced to 2.3.

The molar ratio of bound galactose per SA was quantified by analyzing the ultrafiltrate of each incubation mixture by a carbohydrate assay. The average bound ratios were 5, 8 and 19 galactose moieties per SA for the incubation ratios of 10, 25 and 50, respectively. SA contains a total of 20 amino groups; 16 lysine amino and 4 terminal amino residues. Therefore, the galactose-to-SA ratio of 50 resulted in near saturation of these amines.

SA and SA-gal samples were radiolabeled with  $^{131}\text{I}$  and injected into rabbits ( $n = 3$  per experiment) for in vivo evaluation. Figure 3A shows the blood clearance of each sample. SA and SA-gal-5 circulated similarly with  $>50\%$  in the blood at 2 hr. SA-gal-8 and SA-gal-19 exhibited faster blood clearance, with  $\sim 30\%$  and  $20\%$  circulating at 2 hr, respectively. Biodistribution results (Fig. 3B) indicate that increasing hepatic uptake correlates with the amount of galactose bound per SA.

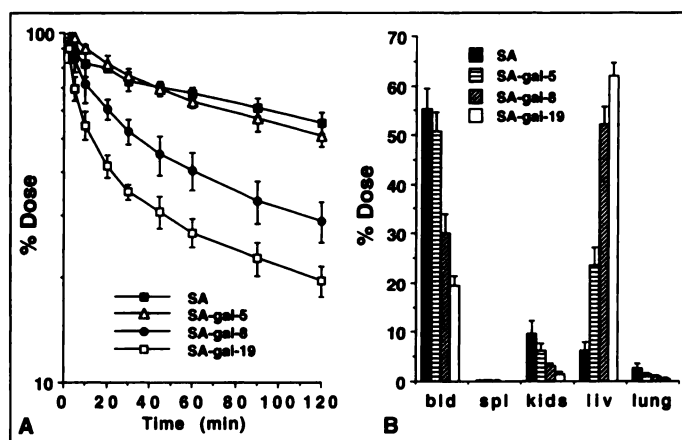


**FIGURE 3.** (A) Blood pharmacokinetics of  $^{131}\text{I}$ -SA and  $^{131}\text{I}$ -SA-gal in the rabbit. (B) Biodistribution of  $^{131}\text{I}$ -SA and  $^{131}\text{I}$ -SA-gal 2 hr after injection in the blood, spleen, kidneys, liver and lung (all data  $n = 3$ ,  $\bar{x} \pm \text{s.d.}$ ).

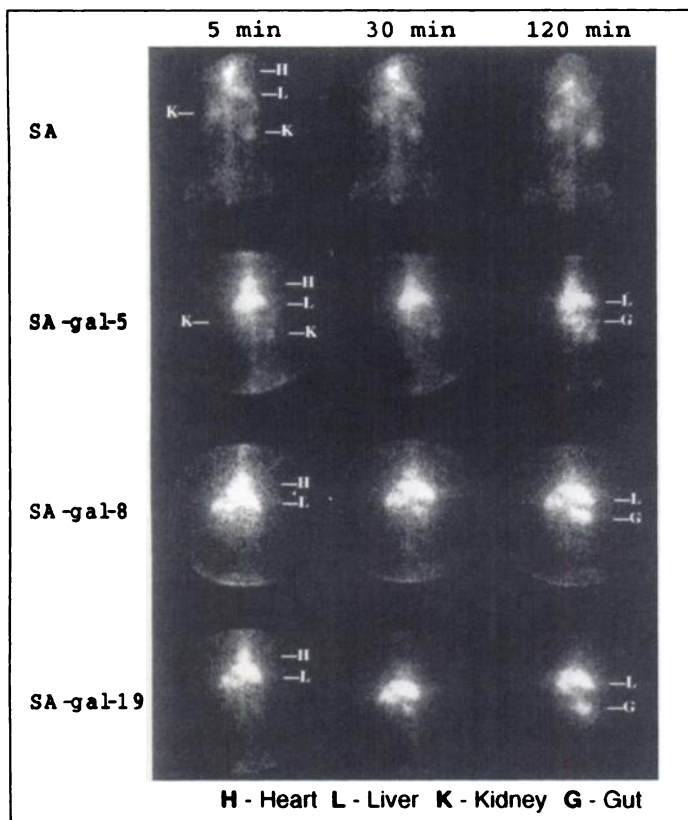


**FIGURE 4.** Nuclear images of of  $^{131}\text{I}$ -SA and  $^{131}\text{I}$ -SA-gal at 5, 30 and 120 min postinjection. Iodine-131 SA imaging showed typical blood flow activity. Iodine-131 SA conjugated with increasing amounts of galactose showed decreased circulatory and increased hepatic activity.

This is consistent with galactose receptor uptake by hepatocytes. Visual results from gamma camera images of rabbits injected with these samples were consistent with the biodistribution results. Iodine-131 SA images (Fig. 4) showed vascular activity as indicated by systemic circulation and cardiac activity. Iodine-131 SA-gal samples showed increasing hepatic uptake and decreased circulation with larger amounts of bound galactose. Hepatic metabolism, as evident by biliary and gut activity, is also present with the  $^{131}\text{I}$ -SA-gal samples in the 30 and 120 min images.

The amino groups of avidin were neutralized by incubation with an N-hydroxysuccinimide ester of acetate (NHS-Ac). Neutralization resulted in a progressive decrease in isoelectric point, corresponding to the incubation ratio of NHS-Ac-to-avidin (Fig. 5A). Avidin was also deglycosylated by endoglycosidase-H digestion (Avid-E). SDS-polyacrylamide electrophoresis (Fig. 5B) of these samples shows that the subunits of avidin and neutralized avidin (Avid-N) had equivalent molec-

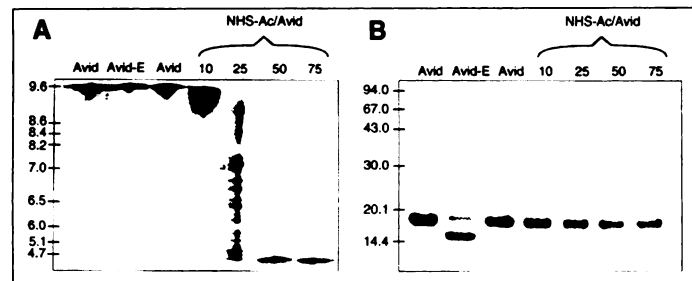


**FIGURE 5.** (A) Isoelectric focusing of avidin and modified avidin shows decrease in isoelectric point of neutralized avidin. (B) SDS polyacrylamide electrophoresis shows a decrease in subunit molecular weight with the removal of oligosaccharide from avidin. Numbers indicate incubation ratios.

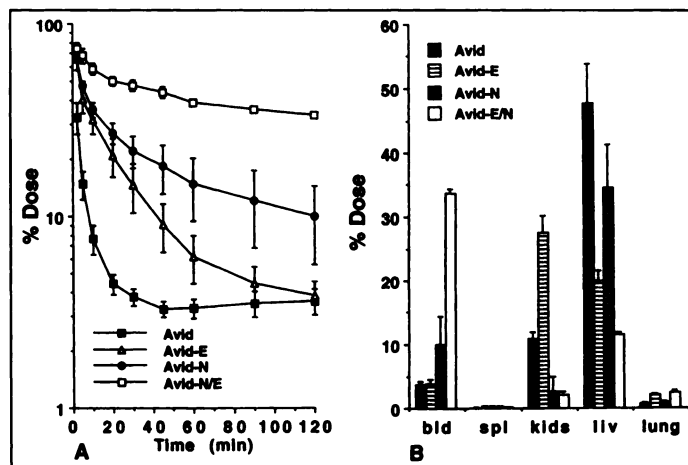


**FIGURE 6.** (A) Blood pharmacokinetics of  $^{131}\text{I}$  avidin and  $^{131}\text{I}$  modified avidin in the rabbit. (B) Biodistribution of  $^{131}\text{I}$  avidin and  $^{131}\text{I}$  modified avidin 2 hr postinjection in the blood, spleen, kidneys, liver and lung (all data  $n = 3$ ,  $\bar{x} \pm$  s.d.).

ular weights; Avid-E, however exhibited decreased molecular weight due to the removal of oligosaccharide. Deglycosylation had no effect on avidin's isoelectric point. DACB saturation analysis (Fig. 2B) resulted in a less than maximum DACB-to-avidin ratio of 2.8 with native avidin. Similar to SA, avidin did not show a decrease in biotin binding until large amounts of lysine neutralization occurred.

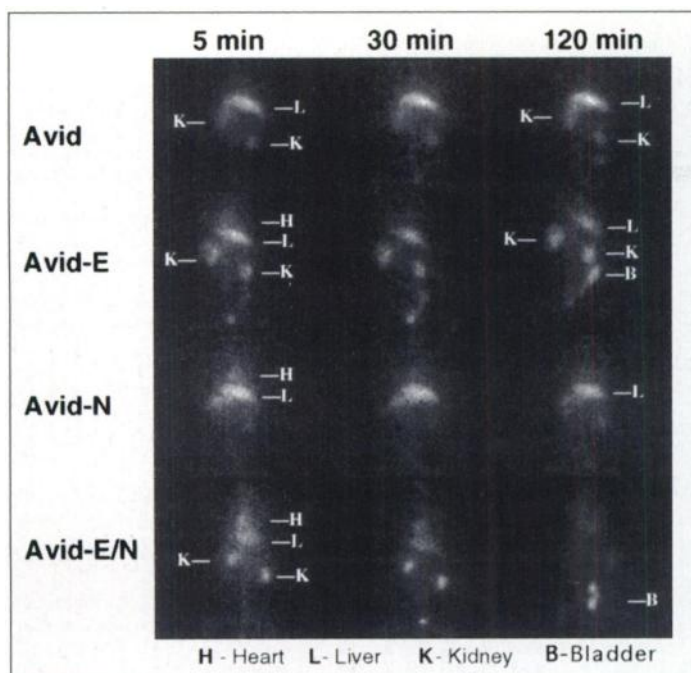
To investigate the effect of modification in vivo, avidin, Avid-E, Avid-N (Avid-N = 50 to 1 NHS-Ac-to-avidin ratio) and Avid-E with neutralization (Avid-E/N) were radiolabeled with  $^{131}\text{I}$  and injected into rabbits ( $n = 3$  per experiment). Iodine-131 avidin cleared quickly from the circulation (Fig. 6A). Iodine-131 Avid-E and  $^{131}\text{I}$  Avid-N cleared slower than native avidin, but still exhibited relatively rapid clearance. The blood clearance of  $^{131}\text{I}$  Avid E/N was substantially prolonged with circulatory values at 2 hr approaching that of  $^{131}\text{I}$  SA. Biodistribution results differed with each type of modification (Fig. 6B). Iodine-131 avidin accumulated mostly in the liver and kidneys. Iodine-131 Avid-E kidney accumulation increased with a corresponding decrease in liver activity. Conversely,  $^{131}\text{I}$  Avid-N kidney accumulation decreased considerably, but had a high liver accumulation. With  $^{131}\text{I}$  Avid E/N, there were low levels in both the kidneys and in the liver. These results suggest that the clearance of avidin consists of two mechanisms, one due to net charge and one resulting from specific sugar receptor binding.

Figure 7 shows  $^{131}\text{I}$ -labeled avidin and modified avidin sample images. Consistent with the biodistribution results,  $^{131}\text{I}$  avidin activity was exclusively in the liver and kidneys. Iodine-131 Avid-E had increased kidney activity. Iodine-131 Avid-N images showed a dramatic reduction in kidney activity that corresponded with an increase in liver activity. Iodine-131 Avid-E/N showed circulatory activity with a corresponding decrease in liver and kidney activity. Urine activity was present with  $^{131}\text{I}$  Avid-E and  $^{131}\text{I}$  Avid-E/N and, when analyzed by Centricon-30 ultrafiltration, >90% of the activity was protein bound.

## DISCUSSION

A common problem associated with the use of directly radiolabeled MAbs in vivo, or their F(ab')<sub>2</sub> and Fab fragments, is high background activity due to their prolonged circulation and accumulation in organs, especially in the liver and the kidneys (26–28). Different immunological approaches utilizing the SA (avidin)/biotin system have been investigated for diag-





**FIGURE 7.** Nuclear images of  $^{131}\text{I}$  avidin and  $^{131}\text{I}$  modified avidin at 5, 30 and 120 min postinjection. Iodine-131 avidin cleared quickly to the liver and kidney. Modified  $^{131}\text{I}$  avidin exhibited slower blood clearance, as evidenced by increased circulatory activity.

nosis and therapy of in vivo lesions (29–34). For cancer imaging, a three-step approach is used that involves biotinylated antibody, followed by avidin or SA and then radiobiotin (29). A pre-targeting approach involves the initial injection of cross-linked SA-MAb for in vitro target accumulation. A biotin conjugated clearing agent is then injected to remove circulating SA-MAB, followed by an injection of radiobiotin (32). These multistep procedures require many days to complete. A two-step approach using SA-MAB has been investigated clinically; due to the long circulatory time of SA-MAB, however, radiobiotin was not administered until 2 to 3 days after SA-MAB injection (31). Moreover, the noncovalent cross-linking of SA to MAB was accomplished by biotinylating the MAB, thereby, reducing the maximum radiobiotin binding capability of SA-MAB. We are developing a rapid two-step procedure using biochemically modified SA or avidin covalently cross-linked (preserving the tetravalent biotin binding) to fibrin-specific MABs (35–37) for the diagnosis of intravascular lesions (e.g., thrombi, emboli and atherosclerosis).

The hepatocyte galactose receptor is selective to galactose sugars on glycoproteins and other macromolecules (6,7). These galactose residues are usually covered by sialic acids. During normal protein turnover, neuraminidase cleaves terminal sialic acids exposing galactose sugars, with the resultant galactose-protein able to bind to hepatocyte receptors. This catabolic system has been thoroughly studied (38,39). Within a few minutes after receptor binding, galactose proteins are internalized and digested in lysosomes. Galactose protein modification has been utilized for a variety of in vivo diagnostic procedures. For example, galactose has been conjugated to radiolabeled MABs for both diagnostic and therapeutic approaches to lower blood activity (21,22) and has also been conjugated to albumin for functional imaging studies of the liver (19,20). Both of these procedures result in radionuclide accumulation in the liver. This is problematic for imaging liver or chest lesions and for therapy due to the catabolic liberation of radionuclides that will increase dosimetry to radiosensitive organs, especially bone marrow.

These issues are not relevant for two-step approaches using SA-gal moieties, since SA-gal is not radiolabeled and since radiobiotin will not accumulate in the liver because of rapid receptor mediated endocytosis.

The in vivo fate of avidin has been investigated by our group and others (10–12). Radiolabeled avidin accumulates extensively in the liver after injection. In a previous study, using  $^{111}\text{In}$  DTPA-biotin/avidin, we reported that ~80% of the injected  $^{111}\text{In}$  activity remained in the liver at 6 hr (12). In this study, we found ~50% accumulation with  $^{131}\text{I}$  avidin at 2 hr. These apparent differences in biodistribution most likely result from a difference in cellular metabolism of the two types of radionuclides. During metabolism, iodine or iodine containing peptides are excreted from the cell, whereas radiometals, such as  $^{111}\text{In}$ , enter the iron pathway and are retained intracellularly (38,39). In this study, the accumulation of avidin in the liver and the kidneys appears to involve two mechanisms, one involving mannose receptor binding, most likely by Kupffer cells, and the other involving nonspecific charge interaction with cellular and basement membranes. When avidin was deglycosylated, a large increase in kidney accumulation resulted. This is most likely due to charge interaction with the glomerular basement membrane. In other studies, avidin and other cationic proteins have been shown to accumulate on the glomerular membrane in vitro and in vivo (40–42). When avidin was deglycosylated and neutralized, liver and kidney activity were substantially reduced and circulatory activity increased. Therefore, both the positive net charge and its carbohydrates play a role in avidin's rapid blood clearance and its accumulation in the liver and kidneys.

## CONCLUSION

SA and avidin exhibit markedly different pharmacokinetics after intravenous injection. For a rapid two-step procedure, SA containing moieties would clear too slowly, thereby delaying the injection of radiobiotin until blood levels have decreased. For avidin, its rapid blood clearance and unfavorable biodistribution make it undesirable for in vivo use. Biochemically modified SA and avidin exhibited favorable pharmacokinetics. Therefore, the use of modified SA or avidin conjugated to targeting moieties, such as MABs, MAB fragments or peptides, may be optimal for two-step imaging and therapeutic procedures.

## REFERENCES

1. Wilchek M, Bayer EA. The avidin-biotin complex in bioanalytical applications. *Anal Biochem* 1988;171:1–32.
2. Green NM. Avidin. *Av Protein Chem* 1975;29:85–133.
3. DeLange RJ. Egg white avidin. I. Amino acid composition; sequence of the amino- and carboxyl-terminal cyanogen bromide peptides. *J Biol Chem* 1970;245:907–916.
4. Bruch RC, White HB. Compositional and structural heterogeneity of avidin glycopeptides. *Biochem* 1982;21:5334–5341.
5. Hiller Y, Gershoni JM, Bayer EA, Wilchek M. Biotin binding to avidin. Oligosaccharide side chain not required for ligand association. *Biochem J* 1987;248:167–171.
6. Hubbard AL, Wilson G, Ashwell G, Stukenbrok H. An electron microscope autoradiographic study of the carbohydrate recognition systems in rat liver. I. Distribution of  $^{125}\text{I}$ -ligands among the liver cell types. *J Cell Biol* 1979;83:47–64.
7. Ashwell G, Harford J. Carbohydrate-specific receptors of the liver. *Ann Rev Biochem* 1982;51:531–554.
8. Townsend R, Stahl P. Isolation and characterization of a mannose/N-acetylglucosamine/fucose binding protein from the rat liver. *Biochem J* 1981;194:209–214.
9. Toth CA, Thomas P. Liver endocytosis and Kupffer cells. *Hepatology* 1992;16:255–266.
10. Pimm MV, Fells HF, Perkins AC, Baldwin RW. Iodine-131 and indium-111-labeled avidin and streptavidin for pretargeted immunoscintigraphy with biotinylated antitumor monoclonal antibody. *Nucl Med Commun* 1988;9:931–941.
11. Schechter B, Silberman VR, Aron R, Wilchek M. Tissue distribution of avidin and streptavidin injected to mice. *Eur J Biochem* 1990;189:327–331.
12. Rosebrough SF. Pharmacokinetics and biodistribution of radiolabeled avidin, streptavidin and biotin. *Nucl Med Biol* 1993;20:663–668.
13. Hnatowich DJ, Virzi F, Rusckowski M. Investigation of avidin and biotin for imaging applications. *J Nucl Med* 1987;28:1294–1302.
14. Virzi F, Fritz B, Rusckowski M, et al. New  $^{111}\text{In}$ -labeled biotin derivatives for improved immunotargeting. *Nucl Med Biol* 1991;18:719–726.

15. Rosebrough SF. Plasma stability and pharmacokinetics of radiolabeled deferoxamine-biotin derivatives. *J Pharm Exp Ther* 1993;265:408-415.
16. del Rosario RB, Wahl RL. Biotinylated iodo-polylysine for pretargeted radiation delivery. *J Nucl Med* 1993;34:1147-1151.
17. Khawli LA, Kassiss AI. m-[<sup>125</sup>I]iodoaniline: a useful reagent for radiolabeling biotin. *Nucl Med Biol* 1992;19:297-301.
18. Shoup TM, Fishman AJ, Jaywook S, et al. Synthesis of fluorine-18-labeled biotin derivatives: biodistribution and infection localization. *J Nucl Med* 1994;35:1685-1690.
19. Vera DR, Stadalnik RC, Krohn KA. Technetium-99m galactosyl-neoglycoalbumin: preparation and preclinical studies. *J Nucl Med* 1985;26:1157-1167.
20. Stadalnik RC, Kudo M, Eckelman WC, Vera DR. In vivo functional imaging using receptor-binding radiopharmaceuticals. *Investig Radiol* 1993;28:64-70.
21. Ong GL, Etnenson D, Sharkey RM, et al. Galactose-conjugated antibodies in cancer therapy: properties and principles of action. *Cancer Res* 1991;51:1619-1626.
22. Mattes MJ. Biodistribution of antibodies after intraperitoneal or intravenous injection and effect of carbohydrate modifications. *JNCI* 1987;79:855-863.
23. Roe JH. The determination of sugar in blood and spinal fluid with anthrone reagent. *J Biol Chem* 1955;212:335-343.
24. Armin J, Grant RT, Pels H, Reeve EB. The plasma cell and blood volume of albino rabbits as estimated by the dye (T 1824) and <sup>32</sup>P-marked cell methods. *J Physiol* 1952;116:59-73.
25. Dittmer DS. Biological handbooks: blood and other body. Federation of American Societies for Experimental Biology, 1961:359.
26. Epenetos AA, Snook D, Durbin H, Johnson PM, Taylor-Papadimitriou J. Limitations of radiolabeled monoclonal antibodies for localization of human neoplasms. *Cancer Res* 1986;46:3183-3191.
27. Hnatowich DJ. Recent developments in the radiolabeling of antibodies with iodine, indium, and technetium. *Semin Nucl Med* 1990;20:80-91.
28. Vaughan ATM, Anderson P, Dykes PW, et al. Limitations to the killing of tumors using radiolabeled antibodies. *Br J Radiol* 1987;60:567-578.
29. Paganelli G, Riva P, Deleide G, et al. In vivo labeling of biotinylated monoclonal antibodies by radioactive avidin: a strategy to increase tumor radiolocalization. *Int J Cancer* 1988;2:121-125.
30. Klibanov AL, Martynov AV, Slinkin MA, et al. Blood clearance of radiolabeled antibody: enhancement by lactosamination and treatment with biotin-avidin or anti-mouse IgG antibodies. *J Nucl Med* 1988;29:1951-1956.
31. Kalofonos HP, Rusckowski M, Siebecker DA, et al. Imaging of tumor in patients with indium-111-labeled biotin and streptavidin-conjugated antibodies: preliminary communication. *J Nucl Med* 1990;31:1791-1796.
32. Goodwin DA, Meares CF, McCall MJ, McTigue M, Chaovapong W. Pretargeted immunoscintigraphy of murine tumors with indium-111-labeled bifunctional haptens. *J Nucl Med* 1988;29:226-234.
33. Paganelli G, Belloni C, Magnani P, et al. Two-step tumor targeting in ovarian cancer patients using biotinylated monoclonal antibodies and radioactive streptavidin. *Eur J Nucl Med* 1992;19:322-329.
34. van Osdol WW, Sung C, Dedrick RL, Weinstein JN. A distribution pharmacokinetic model of two-step imaging and treatment protocols application to streptavidin-conjugated monoclonal antibodies and radiolabeled biotin. *J Nucl Med* 1993;34:1552-1564.
35. Rosebrough SF, Kudryk BJ, Grossman ZD, et al. Radiomunoimaging of venous thrombi using <sup>131</sup>I-labeled fibrin-specific monoclonal antibody. *Radiology* 1985;156:515-517.
36. Rosebrough SF, Grossman ZD, McAfee JG, et al. Thrombus imaging with <sup>111</sup>In- and <sup>131</sup>I-labeled fibrin-specific monoclonal antibody and F(ab')<sub>2</sub> and Fab fragments. *J Nucl Med* 1988;29:1212-1222.
37. Rosebrough SF, McAfee JG, Grossman, et al. Thrombus imaging: a comparison of radiolabeled GC4 and T2G1s fibrin-specific monoclonal antibodies. *J Nucl Med* 1990;31:1048-1054.
38. Hubbard AL, Stukenbrok H. An electron microscope autoradiographic study of the carbohydrate recognition systems in rat liver. II. Intracellular fates of the <sup>125</sup>I-ligands. *J Cell Biol* 1979;83:65-81.
39. LaBadie JH, Chapman KP, Aronson JN. Glycoprotein catabolism in rat liver. *Biochem J* 1975;152:271-279.
40. Vogt A, Rohrbach R, Shimizu F, Takamiya H, Batsford S. Interaction of cationized antigen with rat glomerular basement membrane: in situ immune complex formation. *Kidney International* 1982;22:27-35.
41. Border WA, Ward HJ, Kamil ES, Cohen AH. Induction of membranous nephropathy in rabbits by administration of an exogenous cationic antigen. *J Clin Invest* 1982;69:451-461.
42. Kaseda N, Uehara Y, Yamamoto Y, Tanaka K. Induction of in situ immune complexes in rat glomeruli using avidin, a native cation macromolecule. *Br J Exp Path* 1985;66:729-736.

## Prevention of Radiolysis of Monoclonal Antibody during Labeling

Munna C. Chakrabarti, Nhat Le, Chang H. Paik, William G. De Graff and Jorge A. Carrasquillo

Department of Nuclear Medicine, Warren G. Magnuson Clinical Center; and Radiation Biology Branch, National Cancer Institute of the National Institutes of Health, Bethesda, Maryland

Monoclonal antibody may undergo loss of immunoreactivity due to radiation damage when labeled with large amounts of <sup>131</sup>I or <sup>90</sup>Y for therapy. Our aim was to develop a method to protect an antibody during the labeling procedure. **Methods:** As a model we used T101, a murine monoclonal antibody directed against CD5 antigen. Iodine-125-T101 (100 µg, 1 ml) was mixed with <sup>90</sup>Y-DTPA (0.64 MBq to 165.9 MBq) for 24 hr in order to deliver doses of 5 Gy to 1280 Gy to the solution. In separate experiments, <sup>125</sup>I-T101 solutions were irradiated with <sup>60</sup>Co external beam delivering radiation doses of 40 Gy to 1280 Gy. The effect of radiation on T101 immunoreactivity was tested by using the CCRF-CEM cell line, and the bound T101 radioactivity was determined. In a final experiment, we directly labeled a DTPA conjugated T101 using 561 MBq of <sup>90</sup>Y under conditions delivering ~640 Gy to the solution. Previously used radioprotectants including human serum albumin, cysteamine and glycerol were evaluated. We focused on ascorbic acid because it is an FDA approved drug that does not interfere with the radiolabeling process. **Results:** The immunoreactivity of <sup>125</sup>I-T101 was ~83%, but at 640 Gy the immunoreactivity decrease to 7%. In contrast, in the presence of radioprotectants this decrease could be abrogated. External irradiation also showed a dose dependent decrease in

immunoreactivity to as low as 0.3% at 1280 Gy. Adding ascorbic acid (5.5 mg/ml) to the solutions prior to the irradiation largely abrogated this decrease. The immunoreactivity of T101 labeled with <sup>90</sup>Y without protectant showed 46% immunoreactivity whereas, in presence of ascorbic acid (11 mg/ml) full retention of immunoreactivity was observed. **Conclusion:** Various radioprotectants can successfully prevent the loss of immunoreactivity or breakdown as a result of radiolysis. Ascorbic acid is an effective radioprotectant that can be used to prevent loss of antibody immunoreactivity during the labeling process.

**Key Words:** monoclonal antibody; labeling damage; immunoreactivity; yttrium-90; radioimmunotherapy; radiolysis

**J Nucl Med** 1996; 37:1384-1388

The use of radiolabeled antibodies as tumor targeting reagents for radioimmunotherapy is under evaluation (1). Several reports treating hematological malignancies with <sup>131</sup>I or <sup>90</sup>Y radiolabeled antibodies have shown promising results (2-4). Several radionuclides have been proposed for radioimmunotherapy including <sup>131</sup>I, <sup>90</sup>Y and <sup>177</sup>Lu (5). These radionuclides deliver a large amount of radiation to the antibody solution during the labeling process as well as during the storage prior to injection. Several reports have confirmed significant damage to antibodies as a result of the labeling and storage (6,7,9,10). The

Received Apr. 14, 1995; revision accepted Aug. 16, 1995.

For correspondence or reprints contact: Jorge A. Carrasquillo, MD, Department of Nuclear Medicine, Clinical Center, National Institute of Health, 10 Center Dr., MSC 1180, Bldg. 10/1C-401, Bethesda, MD 20892-1180.